

Phenomenological theory of current driven exchange switching in ferromagnetic nanojunctions

E. M. Epshtein, Yu. V. Gulyaev, and P. E. Zilberman*

*Institute of Radio Engineering and Electronics of the Russian Academy of Sciences,
Fryazino, Moscow Region, 141190, Russia*

(Dated: October 26, 2018)

Phenomenological approach is developed in the theory of spin-valve type ferromagnetic junctions to describe exchange switching by current flowing perpendicular to interfaces. Forward and backward current switching effects are described and they may be principally different in nature. Mobile electron spins are considered as free in all the contacting ferromagnetic layers. Joint action of the following two current effects is investigated: the nonequilibrium longitudinal spin-injection effective field and the transverse spin-transfer surface torque. New vector boundary conditions are derived, which represent, in essence, the continuity condition for different spin fluxes. Dispersion relation for fluctuations is derived and solved for a junction model having spatially localized spin transfer torque: depth of the torque penetration into the free layer is assumed much smaller than the total free layer thickness. Some critical value κ_0 of the well known Gilbert damping constant κ is established for the first time. Spin transfer torque dominates in the instability threshold determination for small enough constants $\kappa < \kappa_0$, while the spin-injection effective field dominates for $\kappa > \kappa_0$. Typical estimation gives $\kappa_0 \sim 3 \times 10^{-2}$ and it shows that the both mechanisms mentioned may be responsible for the observable threshold in ferromagnetic metal free layer used at room temperature. Fine interplay between spin transfer torque and spin injection is necessary to provide a hysteretic behavior of the resistance versus current dependence. The state diagrams building up show the possibility of non-stationary (time dependent) nonlinear states arising due to instability development. Calculations lead to the instability increment values of the order of $\lesssim 10^{10} \text{ s}^{-1}$ and they are really containing the contributions from the two mechanisms mentioned. Spin wave resonance frequency spectrum softening occurs under the current growing to the instability threshold. Magnetization fluctuations above the threshold rise oscillatory with time for small damping ($\kappa < \kappa_0$), but rise aperiodically and much more rapid for large damping ($\kappa > \kappa_0$).

PACS numbers: 72.25.Ba, 72.25.Hg, 75.47.-m

I. INTRODUCTION

Spin valve type magnetic junctions are of very interest for investigations and subsequent applications. A number of significant effects were predicted and experimentally revealed in the junctions last years. Magnetization instability was predicted in Refs. 1,2. The instability is driven by the current perpendicular to plane (CPP regime) due to near interface transformation of a transverse part of mobile electron spin flux to the lattice magnetization flux. This mechanism is usually referred to as a surface *transverse spin transfer* (TST) torque. Another mechanism was proposed and theory elaborated in Refs. 3,4,5,6. This second mechanism is due to nonequilibrium *longitudinal spin injection* (LSI) by current into the bulk of a ferromagnetic layer. The injected spins create current dependent *sd* exchange in nature effective field, which acts on the lattice magnetization and may stimulate reorientation phase transition. Theory of the joint action of the two mechanisms mentioned was developed recently⁷ (see also preprints^{8,9} and Ref. 10).³⁸

Current driven instability was revealed experimentally, being manifested in resistance jumps¹¹ and in microwave emission.¹² Many interesting subsequent experiments confirmed the first observations in principle and gave a lot of additional significant information (see, e.g., Refs. 13,14,15,16,17,18). The most of experiments con-

sidered trilayers Co/Cu/Co as a constitutive working part of the junction. The first Co layer has usually pinned lattice due to large its own thickness or existence of additional pinning layers. The second Co layer is taken thin enough to have free lattice magnetization, which may be controlled by external field or current. It is significant to remark that thickness L of the second free layer cannot be done less than $\sim 2 \text{ nm}$ to prevent a non-continuous structure appearing.¹¹ Typically, the thicknesses in experiments were chosen within the range $L \sim 2.5\text{--}10 \text{ nm}$.

Success in experimental study and in applications stimulated an activity to achieve more detailed understanding of the fundamental idea of TST process introduced in Refs. 1,2. Contrary to this, in the present paper we accept this idea without any additional proof: an abrupt transformation appears of transverse mobile electron spin flux to the lattice magnetization flux at the interface between the layers. Great attention was paid already to justify this idea more rigorously starting from the microscopy theory approach (see, e.g., Refs. 19,20,21,22,23,24). However, the phenomenological approach is necessary also because of its more wide sight.

Exactly such an approach we laid in the basis of the present paper. In other words, we accept the mobile electrons cannot perform long time and long distance precession around the lattice magnetization because of phase

mismatch of individual electrons due to their statistical velocity spread.^{1,2} As a result, the transverse component of the mobile electron magnetization vector decays rapidly and transfers to the lattice of ferromagnet. This picture is taken as the base of our consideration and then all the phenomenology is built up.

Such an approach allows us to integrate in the theory the second mechanism of current action that is LSI. Therefore the LSI effective field and TST torque are treated simultaneously as the two manifestations of the only *sd* exchange interaction. Additionally, we shall show such significant effects as the backward current switching and the hysteretic resistance versus current dependence may be understood as a fine interplay of the two mechanisms mentioned. As far as we know, similar unified description including the both mechanisms, TST and LSI, could not be developed yet in the frame of a microscopic theory. Moreover, we calculate in the present paper not only the threshold current (that was done in many papers) but the property of the various magnetic configurations: what configurations remain stable and what ones become unstable depending on the current. Similar experimental data were presented in the literature before and we have now a possibility to compare some of them with the theory. We show (similar to Refs. 7,8) the spin wave spectrum of the junction layer should soften to zero under the current is growing and tends to the instability threshold. That is decisive manifestation of the LSI mechanism, which specifies it in comparison with the TST one. We estimate also the rise time for the unstable fluctuations. The minimal rise time may be less than ~ 0.1 ns but only if the LSI mechanism of instability is dominated.

Let us make some more preliminary remarks. The first remark concerns to the model of the system under consideration. According to the original estimations^{1,2} and subsequent theory calculations,^{19,20,21,23} the depth of transverse spin flux penetration into the free layer is of the order of electron quantum wavelength at the Fermi surface $\lambda_F \lesssim 1\text{--}3$ nm and is strongly nonuniform within this interval. The spin transfer torque acts, as it is well known,^{1,2} in that interval only. Therefore the uniform approximation of the torque throughout the whole thickness L seems to be very approximate at least for large enough $L \gtrsim 4\text{--}10$ nm. Because of the model of the torque, which is uniformly spread in the free layer, is traditional one, it needs, at least, to be justified. Recently^{7,8,9} we proposed another model for the calculations, namely, to consider spin transfer torque as a boundary condition at the pinned/free layer interface. In essence, this model is an opposite limiting case with respect to the uniform torque model. The obvious advantage of our model is in its complete non-sensitivity to details of the processes inside the sublayer adjusted to the interface and having thickness λ_F . More detailed comparison of these two models will be discussed in Appendix.

The second remark concerns to the external magnetic field influence. We assume the junction may be placed in

some external magnetic field \mathbf{H} , which lies in the plane of junction interfaces. But this field is supposed to be less in magnitude in comparison with the layer magnetic anisotropy field H_a , that is $|\mathbf{H}| \equiv H < H_a$. Such a supposition is accepted for simplicity because we want focus our attention here to current (not to field) driven magnetization reversal processes. Recent papers^{25,26} show at large enough fields $H \geq 4\pi M \gg H_a$ the situation may become much more complicated.

II. MODEL CONSIDERED

We will use further the most elementary model of a ferromagnetic metal based on the well known concept of free *s*-electron (quasiparticle) ideal gas interacting with the lattice³⁹ bound *d*-electron magnetization due to the so called *sd* exchange interaction.²⁷ Some more advanced (and more complicated!) models may be used, of course. However, on our opinion, the most actual problem now is to explain a number of experimental facts concerning to switching of ferromagnetic nanojunctions. We believe it may be done in the frame of the simple model.⁴⁰

We assume the junction consists of two ferromagnetic metal layers and one very thin nonmagnetic spacer in between (shown as a heavy line in Fig. 1). To close the electric circuit, a nonmagnetic metal layer **3** is necessary. The ferromagnetic metal layer **1** has pinned orientation of the lattice magnetization \mathbf{M}_1 , but the mobile electron magnetization \mathbf{m}_1 is, in general, non-pinned. Another ferromagnetic metal layer **2** has free lattice magnetization \mathbf{M}_2 and mobile electron magnetization \mathbf{m}_2 , so that the magnetizations direction can be changed by an external magnetic field \mathbf{H} or spin-polarized current density \mathbf{j} .

Plane $x = 0$ is the interface between the layers **1** and **2** and lattice magnetization \mathbf{M}_1 lies within the plane. Vectors \mathbf{M}_1 and \mathbf{M}_2 make an angle χ of an arbitrary value under the current is absent, that is under $\mathbf{j} = 0$. After the current is turned on, the electrons flow from the layer **1** into the layer **2** or vice versa and then appear in a non-stationary quantum state and “walk” between the spin energy subbands of the corresponding layer. For forward current, when the inequality $j/e > 0$ is valid, vectors \mathbf{m}_2 and \mathbf{M}_2 perform a precession (see Fig. 1). As it was shown first in Refs. 1,2, angle of the precession decreases with coordinate x increasing and tends to zero at $x \approx \lambda_F$, where λ_F is an electron quantum wavelength at the Fermi surface. This is because of electron velocity statistical spread and no relaxation processes are needed to provide such a behavior. More detailed discussion may be found also in the recent preprint.⁸ Analogous “precession” region appears, of course, near the interface $x = 0$ for backward electron current, that is for $j/e < 0$. However, the region will be localized not in the layer **1** but again in the region $0 < x < \lambda_F$ of the layer **2**. It appears due to the complete pinning of the lattice in the layer **1**. This feature is better to discuss a little below in the paper.

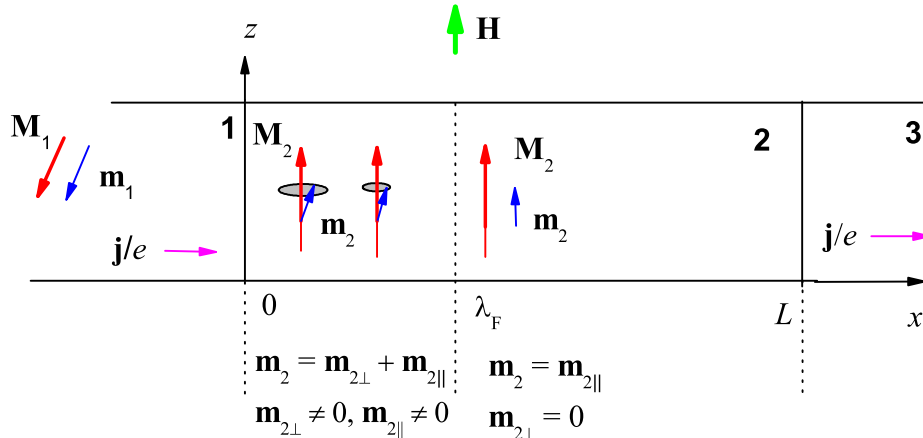


FIG. 1: (Color online) A scheme of magnetic junction to illustrate processes in layer **2**. The contacting layers are labelled by **1**, **2**, **3**. The arrows show directions of the following vectors: \mathbf{M}_1 and \mathbf{m}_1 are magnetizations in the layer **1**, \mathbf{M}_2 and \mathbf{m}_2 are magnetizations in the layer **2**, external magnetic field \mathbf{H} lies in the junction plane $x = 0$, and current density is \mathbf{j}/e (e is electron charge). The vertical dashed lines separate two ranges in the layer **2**. In $0 \leq x \leq \lambda_F$ range, precession takes place, which is shown with ovals. Vector \mathbf{m}_2 has both longitudinal and transverse components $\mathbf{m}_{2\parallel}$ and $\mathbf{m}_{2\perp}$, respectively. The precession angle decreases with x increasing. In $x > \lambda_F$ range, the precession vanishes, so that only the longitudinal component remains.

The region $0 < x < \lambda_F$ was introduced firstly by Slonczewski¹ and Berger² and further we will refer to it as “SB layer”. Their considerations of the layer were based on the assumption that a ballistic transport occurs inside. An opposite limiting case, when diffusion transport dominates, was considered in Refs. 19,23. We follow, in this point, the approach of the original works.^{1,2} The validity criterion for this assumption may be written as $\lambda_F < l_p$, where momentum mean free pass length l_p may be estimated as $\sim 1\text{--}10$ nm for metals at room temperature. As for the region $x > \lambda_F$ in the layer **2**, the length l_p appears indeed very small one. Based on this reason, we will consider further the electron transport outside the SB layer (in the depth of the layer **2**) using the diffusion–drift limit.

III. LATTICE EQUATIONS OF MOTION

Quantities that have no number indexes (1, 2 or 3) we refer further to any of the junction layers. Motion of vector \mathbf{M} will be described by means of the Landau–Lifshitz–Gilbert (LLG) continuity equation:

$$\frac{\partial \mathbf{M}}{\partial t} + \gamma [\mathbf{M}, \mathbf{H}_{eff}] - \frac{\kappa}{M} \left[\mathbf{M}, \frac{\partial \mathbf{M}}{\partial t} \right] = 0, \quad (1)$$

where t is time, γ is the gyromagnetic ratio, κ is dimensionless lattice damping constant ($0 < \kappa \ll 1$),

$$\mathbf{H}_{eff} = \mathbf{H} + \mathbf{H}_a + A \frac{\partial^2 \mathbf{M}}{\partial x^2} + \mathbf{H}_d + \mathbf{H}_{sd} \quad (2)$$

is effective field, $\mathbf{H}_a = \beta(\mathbf{M}\mathbf{n})\mathbf{n}$ is anisotropy field, β being dimensionless anisotropy constant (typically, $\beta \sim 0.1$ for our magnets) and \mathbf{n} being a unit vector along the anisotropy axis direction, A is the intralattice inhomogeneous exchange constant (magnetic “stiffness” of the lattice), \mathbf{H}_d is demagnetization field, \mathbf{H}_{sd} is sd exchange effective field. The latter takes the form²⁸

$$\mathbf{H}_{sd}(x) = -\frac{\delta U_{sd}}{\delta \mathbf{M}(x)}, \quad (3)$$

where $\delta(\dots)/\delta \mathbf{M}(x, t)$ is a variational derivative, and U_{sd} is sd exchange energy,

$$U_{sd} = -\alpha_1 \int_{-\infty}^0 \mathbf{m}_1(x') \mathbf{M}_1 dx' - \alpha_2 \int_0^L \mathbf{m}_2(x') \mathbf{M}_2(x') dx', \quad (4)$$

parameters α_1 and α_2 being dimensionless sd exchange constants (typical estimations are $\alpha_1 \sim \alpha_2 \sim 10^4\text{--}10^6$). Due to the last term in Eq. (2), the motion of vectors \mathbf{M}_2 , \mathbf{m}_1 and \mathbf{m}_2 appears to be coupled. Remember, vector \mathbf{M}_1 is pinned completely in our model and cannot be moved.

IV. SPATIAL DISTRIBUTION OF MOBILE ELECTRON MAGNETIZATION

We describe the motion of vector \mathbf{m} by means of continuity equation

$$\frac{\partial \mathbf{m}}{\partial t} + \frac{\partial \mathbf{J}}{\partial x} + \gamma \alpha [\mathbf{m}, \mathbf{M}] + \frac{\mathbf{m} - \bar{\mathbf{m}}}{\tau} = 0, \quad (5)$$

where τ is a time of relaxation to the local equilibrium value $\bar{\mathbf{m}} \equiv \bar{m} \hat{\mathbf{M}}$, $\hat{\mathbf{M}} \equiv \mathbf{M}/M$ is the unit vector, \mathbf{J} is a mobile electron magnetization flux density. We do not consider here the almost ballistic quantum mechanical motion of the mobile electrons inside the SB layer. Instead, we consider the influence of this small thickness layer on the motion outside it by means of an appropriate boundary condition (see below). Diffusion-drift approximation is applicable in the regions outside SB layer, that is for $x > \lambda_F$. The equation (5) may be simplified significantly in this region.

First, only longitudinal part $\mathbf{m}_{\parallel} = m \hat{\mathbf{M}}$ may be taken into account. Therefore an effective frequency ω of the motion is determined by the precession in relatively small fields $H, H_d, \beta M \ll \gamma \alpha M \equiv \omega_{sd} \sim 3 \times 10^{14} \text{ s}^{-1}$. We assume the condition

$$\omega \tau \ll 1 \quad (6)$$

is valid, which allows us to neglect time derivative in Eq. 5 in comparison with the relaxation term. The remaining equation (5) may be solved then with respect to $\Delta \mathbf{m} \equiv (\mathbf{m} - \bar{\mathbf{m}}) = \Delta m \hat{\mathbf{M}}$. Let us take the typical parameter estimations: $\alpha_1 \sim \alpha_2 \sim 2 \times 10^4$, $M \sim 1 \times 10^3 \text{ G}$, $\tau \sim 3 \times 10^{-13} \text{ s}$ to justify the following simplifying condition:

$$\omega_{sd} \tau \sim 10^2 \gg 1. \quad (7)$$

Then Eq. (5) acquires the form

$$\Delta \mathbf{m} = -\tau \hat{\mathbf{M}} \left(\hat{\mathbf{M}} \cdot \partial \mathbf{J} / \partial x \right). \quad (8)$$

Second, spin flux \mathbf{J} can be found explicitly in the region $x > \lambda_F$ to substitute it into Eq. (8). Electrons in the region occupy energy subbands having their own spin magnetic moments parallel to $\hat{\mathbf{M}}$ (\uparrow) and antiparallel to $\hat{\mathbf{M}}$ (\downarrow). Magnetization of the mobile electrons \mathbf{m} contains contributions from the both subbands and therefore may be presented as

$$\mathbf{m} = \mu_B (n_{\uparrow} - n_{\downarrow}) \hat{\mathbf{M}} \equiv m \hat{\mathbf{M}}, \quad (9)$$

where $\mu_B > 0$ is Bohr magneton, $n_{\uparrow, \downarrow}$ are partial electron densities in the spin subbands. The total electron density $n = n_{\uparrow} + n_{\downarrow}$ does not depend on x and t because of local neutrality conditions in metal. The magnetization flux density \mathbf{J} in Eq. (8) also can be related with partial electric current densities in each subbands, j_{\uparrow} and j_{\downarrow} . The relation has the following form:

$$\mathbf{J} = \frac{\mu_B}{e} (j_{\uparrow} - j_{\downarrow}) \hat{\mathbf{M}}. \quad (10)$$

The total current density $j = j_{\uparrow} + j_{\downarrow}$ does not depend on x too, because of one-dimensional geometry of our model. We use standard diffusion-drift formula for partial currents:

$$j_{\uparrow, \downarrow} = e n_{\uparrow, \downarrow} \mu_{\uparrow, \downarrow} E - e D_{\uparrow, \downarrow} \frac{\partial n_{\uparrow, \downarrow}}{\partial x}, \quad (11)$$

where $\mu_{\uparrow, \downarrow}$ are partial mobilities, $D_{\uparrow, \downarrow}$ are partial diffusion coefficients and E is an electric field strength inside the layer. Now, we should substitute formula (11) in Eq. (10) and express \mathbf{J} via \mathbf{m} , using Eq. (9). The calculations are direct and were done completely in Ref. 5. The result may be written as follows:

$$\mathbf{J} = \left(\frac{\mu_B}{e} Q j - \tilde{D} \frac{\partial m}{\partial x} \right) \hat{\mathbf{M}}, \quad (12)$$

where $Q = (\sigma_{\uparrow} - \sigma_{\downarrow}) / (\sigma_{\uparrow} + \sigma_{\downarrow})$ may be understood as an equilibrium conductivity spin polarization parameter with $\sigma_{\uparrow, \downarrow} \equiv e n_{\uparrow, \downarrow} \mu_{\uparrow, \downarrow}$, and $\tilde{D} = (\sigma_{\uparrow} D_{\downarrow} + \sigma_{\downarrow} D_{\uparrow}) / (\sigma_{\uparrow} + \sigma_{\downarrow})$ is the effective spin diffusion constant. To obtain Eq. (12), an additional assumption should be made,⁵ namely

$$\frac{j}{j_D} \ll 1, \quad (13)$$

where $j_D \equiv e n l / \tau$ is a characteristic current density in the layer **2**. With typical parameter values, $n \sim 10^{22} \text{ cm}^{-3}$, $l \sim 3 \times 10^{-6} \text{ cm}$, $\tau \sim 3 \times 10^{-13} \text{ s}$, we get $j_D \sim 1.6 \times 10^{10} \text{ A/cm}^2$. The condition means the current disturbs the subband populations rather slightly, so that only a low injection level is realized. As it was mentioned above, we are interesting in currents $j \leq 10^7 - 10^8 \text{ A/cm}^2$, which have an order of instability thresholds. Therefore, the condition (13) should be well satisfied in our calculations.

After substituting expression (12) into Eq. (8) we obtain finally the following equation for m :

$$\frac{\partial^2 m}{\partial x^2} - \frac{\Delta m}{l^2} = 0, \quad (14)$$

where $\Delta m = m - \bar{m}$. Since the sd exchange gap is fixed in our model, \bar{m} value does not depend on x and t . The spin diffusion length is $l = \sqrt{\tilde{D} \tau}$.

As it was mentioned at the beginning of this section, our above presented derivation may be referred to any junction layer. Therefore, Eq. (14) is valid to describe any definite layer if we perform the replacements: $m \rightarrow m_{1,2,3}$, $\hat{\mathbf{M}} \rightarrow \hat{\mathbf{M}}_{1,2,3}$, $Q \rightarrow Q_{1,2,3}$, $\tilde{D} \rightarrow \tilde{D}_{1,2,3}$, $\tau \rightarrow \tau_{1,2,3}$, and so on. Moreover, we should take $\hat{\mathbf{M}}_3 \equiv \hat{\mathbf{M}}_2$, $\bar{m}_3 = 0$, $Q_3 = 0$ for nonmagnetic layer **3** (see Ref. 5 for more details).

To solve Eq. (14), we should derive the appropriate boundary conditions. We accept two sorts of the conditions: 1) the continuity condition of the mobile electron longitudinal spin fluxes, penetrating through the interfaces and 2) the continuity condition for difference between the chemical potentials of electrons in

the spin subbands. It means the following equalities are to be valid for current flowing in forward direction ($j/e > 0$): $\mathbf{J}_1(-\lambda_F)\hat{\mathbf{M}}_2(\lambda_F) = \mathbf{J}_2(\lambda_F)\hat{\mathbf{M}}_2(\lambda_F)$ and $\mathbf{J}_2(L-\varepsilon)\hat{\mathbf{M}}_2(L-\varepsilon) = \mathbf{J}_3(L+\varepsilon)\hat{\mathbf{M}}_2(L-\varepsilon)$, as well the following equalities are to be valid for backward direction of current ($j/e < 0$): $\mathbf{J}_2(\lambda_F)\hat{\mathbf{M}}_1 = \mathbf{J}_1(-\lambda_F)\hat{\mathbf{M}}_1$ and $\mathbf{J}_3(L+\varepsilon)\hat{\mathbf{M}}_2(L-\varepsilon) = \mathbf{J}_2(L-\varepsilon)\hat{\mathbf{M}}_2(L-\varepsilon)$. It may be written in an explicit form using the definition (12):

$$\begin{aligned} & \left(\frac{\mu_B}{e} Q_1 j - \tilde{D}_1 \frac{\partial m_1}{\partial x} \Big|_{x=-\lambda_F} \right) \left(\hat{\mathbf{M}}_1 \hat{\mathbf{M}}_2(\lambda_F) \right) \\ &= \frac{\mu_B}{e} Q_2 j - \tilde{D}_2 \frac{\partial m_2}{\partial x} \Big|_{x=\lambda_F}, \\ & \frac{\mu_B}{e} Q_2 j - \tilde{D}_2 \frac{\partial m_2}{\partial x} \Big|_{x=L-\varepsilon} = -\tilde{D}_3 \frac{\partial m_3}{\partial x} \Big|_{x=L+\varepsilon} \end{aligned} \quad (15)$$

for $j/e > 0$ and

$$\begin{aligned} & \left(\frac{\mu_B}{e} Q_2 j - \tilde{D}_2 \frac{\partial m_2}{\partial x} \Big|_{x=\lambda_F} \right) \left(\hat{\mathbf{M}}_1 \hat{\mathbf{M}}_2(\lambda_F) \right) \\ &= \frac{\mu_B}{e} Q_1 j - \tilde{D}_1 \frac{\partial m_1}{\partial x} \Big|_{x=-\lambda_F}, \\ & -\tilde{D}_3 \frac{\partial m_3}{\partial x} \Big|_{x=L+\varepsilon} = \frac{\mu_B}{e} Q_2 j - \tilde{D}_2 \frac{\partial m_2}{\partial x} \Big|_{x=L-\varepsilon} \end{aligned} \quad (16)$$

for $j/e < 0$.

The continuity condition for chemical potential differences was considered before us but, apparently, only for collinear orientations of magnetizations on the two opposite sides of the boundary (spacer²⁹ or domain wall³⁰). We have written the condition for oblique magnetization orientations in Ref. 31. Now, we should return to the situation of oblique magnetizations because: 1) the idealization of pinned mobile electrons is removed and 2) vectors \mathbf{M}_1 and \mathbf{M}_2 may appear noncollinear. After cal-

culations analogous to Ref. 31, we obtain

$$\begin{aligned} N_1 \Delta m_1(-\lambda_F) &= N_2 \Delta m_2(\lambda_F) \left(\hat{\mathbf{M}}_1 \hat{\mathbf{M}}_2(\lambda_F) \right), \\ N_2 \Delta m_2(L-\varepsilon) &= N_3 \Delta m_3(L+\varepsilon) \end{aligned} \quad (17)$$

for $j/e > 0$ and

$$\begin{aligned} N_1 \Delta m_1(-\lambda_F) \left(\hat{\mathbf{M}}_1 \hat{\mathbf{M}}_2(\lambda_F) \right) &= N_2 \Delta m_2(\lambda_F), \\ N_3 \Delta m_3(L+\varepsilon) &= N_2 \Delta m_2(L-\varepsilon) \end{aligned} \quad (18)$$

for $j/e < 0$. Here the following definitions are introduced: $N = (2\mu_B)^{-1} [(g_\uparrow(\bar{\zeta}))^{-1} + (g_\downarrow(\bar{\zeta}))^{-1}]$, the quantities $g_{\uparrow,\downarrow}$ are densities of states for spin up and spin down electrons, $\bar{\zeta}$ is equilibrium chemical potential, which is constant across each junction layer.

The equation (14) may be directly solved with the following result:

$$\begin{aligned} \Delta m_1(x) &= \tilde{m}_1 \exp\left(\frac{x}{l_1}\right), \\ \Delta m_2(x) &= \tilde{m}_2 \cosh\left(\frac{x}{l_2}\right) + l_2 \tilde{m}'_2 \sinh\left(\frac{x}{l_2}\right), \\ \Delta m_3(x) &= \tilde{m}_3 \exp\left(\frac{L-x}{l_3}\right), \end{aligned} \quad (19)$$

where four constants \tilde{m}_1 , \tilde{m}_2 , \tilde{m}'_2 , \tilde{m}_3 should be found from the boundary conditions (15)–(18). Moreover, we take $\Delta m_1 \rightarrow 0$, $\Delta m_3 \rightarrow 0$ far from the interfaces, that is for $|x| \rightarrow \infty$. Then we obtain the distribution of mobile electron magnetization across the junction considered. After some direct calculations, we obtain the following results for the forward current $j/e > 0$:

$$\begin{aligned} \tilde{m}_2 &= \mu_B n_2 \frac{j}{j_{D2}} \left\{ Q_2 + \left[Q_1 \left(\hat{\mathbf{M}}_1 \hat{\mathbf{M}}_2(\lambda_F) \right) - Q_2 \right] (\cosh \lambda + \nu_2 \sinh \lambda) \right\} \\ &\times \left[\sinh \lambda + \nu_2 \cosh \lambda + \frac{1}{\nu_1} \left(\hat{\mathbf{M}}_1 \hat{\mathbf{M}}_2(\lambda_F) \right)^2 (\cosh \lambda + \nu_2 \sinh \lambda) \right]^{-1}, \end{aligned} \quad (20)$$

$$l_2 \tilde{m}'_2 = \frac{1}{\nu_1} \left(\hat{\mathbf{M}}_1 \hat{\mathbf{M}}_2(\lambda_F) \right)^2 \tilde{m}_2 - \mu_B n_2 \frac{j}{j_{D2}} \left[Q_1 \left(\hat{\mathbf{M}}_1 \hat{\mathbf{M}}_2(\lambda_F) \right) - Q_2 \right], \quad (21)$$

$$\tilde{m}_1 = \frac{N_2}{N_1} \left(\hat{\mathbf{M}}_1 \hat{\mathbf{M}}_2(\lambda_F) \right) \tilde{m}_2. \quad (22)$$

Here we introduce dimensionless thickness $\lambda = L/l_2$ and matching parameters for different interfaces $\nu_1 = \tilde{D}_2 l_1 N_1 / \tilde{D}_1 l_2 N_2$, $\nu_2 = \tilde{D}_3 l_2 N_2 / \tilde{D}_2 l_3 N_3$.

Matching parameters are, in essence, the ratios of corresponding spin contact resistances. For small parameters ($\nu_{1,2} \ll 1$) spin flux penetrates slowly through

the corresponding interface, that is the injection weakens greatly. Similar situation is typical for metal-semiconductor boundary (see, e.g., Ref. 32). Opposite case of large enough parameter ($\nu_{1,2} \gg 1$) corresponds to ready flux penetration through the interface, and the moderate penetration corresponds to $\nu_{1,2} \approx 1$.

As it is seen clearly from formulae (19)–(22), the current disturbs spin equilibrium deeply inside the junction layers at distances of the order of diffusion lengths $l_{1,2,3}$. Therefore the nonequilibrium spin injection by current is indeed a bulk effect. Moreover, the spin injection⁴¹ depends on the angle between the vectors $\hat{\mathbf{M}}_1$ and $\hat{\mathbf{M}}_2(\lambda_F)$. It shows explicitly the mobile electron magnetization does depend on the lattice magnetization vector $\hat{\mathbf{M}}_2$ direction. In principal, such dependence arises because the mobile electrons represent much more rapid system than the magnetic lattice. Therefore the electrons “see” at any time the instantaneous lattice configuration and are adapted to it. Formally, it is seen from our transformation (8) of the basic equation (5) for electrons. The transformation is based on the condition (6). The latter condition allows neglecting any inertia in the electron

following the lattice.

Note finally according to boundary conditions (15)–(18), we may simply make a replacement

$$\left(\hat{\mathbf{M}}_1\hat{\mathbf{M}}_2(\lambda_F)\right) \rightarrow \left(\hat{\mathbf{M}}_1\hat{\mathbf{M}}_2(\lambda_F)\right)^{-1} \quad (23)$$

to go from the forward to backward current direction. Therefore, formulae (19) and (20)–(22) remain valid for backward current ($j/e < 0$) after the replacement (23) is done.

V. CALCULATION OF CURRENT DEPENDENT *SD* EXCHANGE EFFECTIVE FIELD $\mathbf{H}_{sd}(j, x)$

We should calculate variational derivative (3) to find the field $\mathbf{H}_{sd}(j, x)$. First, we calculate the *sd* exchange energy substituting formulae (19)–(22) into expression (4) and performing the integration over coordinate x . Then, we obtain for the forward current ($j/e > 0$)

$$\begin{aligned} U_{sd} = & U_{sd}^{(eq)} - \mu_B \alpha_2 n_2 M_2 l_2 Q_1 \frac{j}{j_{D2}} \left[\sinh \lambda + \nu_2 \cosh \lambda + \frac{1}{\nu_1} \left(\hat{\mathbf{M}}_1 \hat{\mathbf{M}}_2(\lambda_F) \right)^2 (\cosh \lambda + \nu_2 \sinh \lambda) \right]^{-1} \\ & \times \left\{ \frac{Q_2}{Q_1} \left[\sinh \lambda + \frac{1}{\nu_1} (\cosh \lambda - 1) \left(\hat{\mathbf{M}}_1 \hat{\mathbf{M}}_2(\lambda_F) \right)^2 \right] + [\sinh \lambda + \nu_2 (\cosh \lambda - 1)] \left[\left(\hat{\mathbf{M}}_1 \hat{\mathbf{M}}_2(\lambda_F) \right) - \frac{Q_2}{Q_1} \right] \right. \\ & \left. + \frac{b}{\nu_1} \left(\hat{\mathbf{M}}_1 \hat{\mathbf{M}}_2(\lambda_F) \right) \left[\frac{Q_2}{Q_1} + \left[\left(\hat{\mathbf{M}}_1 \hat{\mathbf{M}}_2(\lambda_F) \right) - \frac{Q_2}{Q_1} \right] (\cosh \lambda + \nu_2 \sinh \lambda) \right] \right\}, \quad (24) \end{aligned}$$

where $U_{sd}^{(eq)}$ is an equilibrium part of the energy, which depends only on modulus M_1 and M_2 . Parameter $b = \alpha_1 \tau_1 M_1 / \alpha_2 \tau_2 M_2$ describes the contribution of the layer **1** into the energy (4). Note, that the exchange energy for backward current ($j/e < 0$) may be easily got from expression (24) by means of the replacement (23).

After differentiating (24) in accordance with (3), the equilibrium part of the effective field is collinear with \mathbf{M} and does not contribute to LLG equation (1). Nonequilibrium part of the field may be written as

$$\begin{aligned} \Delta \mathbf{H}_{sd} = & - \frac{\partial U_{sd}}{\partial \left(\hat{\mathbf{M}}_1 \hat{\mathbf{M}}_2(\lambda_F) \right)} \cdot \frac{\delta \left(\hat{\mathbf{M}}_1 \hat{\mathbf{M}}_2(\lambda_F) \right)}{\delta \mathbf{M}_2(x)} \\ = & h_{sd} \hat{\mathbf{M}}_1 l_2 \delta(x - \lambda_F), \quad (25) \end{aligned}$$

where explicit expressions for the field h_{sd} depend on results of differentiation of the energy being different for forward and backward currents. The most general expressions may be directly obtained but appear too cumbersome. We show therefore some simple partial cases only:

a) forward current ($j/e > 0$) and a very thin layer **2** ($\lambda \ll 1$)

$$\begin{aligned} h_{sd} = & \mu_B \alpha_2 n_2 Q_1 \frac{j}{j_{D2}} \left[\nu + \left(\hat{\mathbf{M}}_1 \hat{\mathbf{M}}_2(\lambda_F) \right)^2 \right]^{-2} \\ & \times \left\{ \lambda \nu_1 \left[\nu - \left(\hat{\mathbf{M}}_1 \hat{\mathbf{M}}_2(\lambda_F) \right)^2 \right] \right. \\ & \left. + 2b\nu \left(\hat{\mathbf{M}}_1 \hat{\mathbf{M}}_2(\lambda_F) \right) \right\}, \quad (26) \end{aligned}$$

where $\nu = \nu_1 \nu_2 = \tilde{D}_3 l_1 N_1 / \tilde{D}_1 l_3 N_3$;

b) backward current ($j/e < 0$) and $\lambda \ll 1$

$$h_{sd} = \mu_B \alpha_2 n_2 Q_1 \frac{j}{j_{D2}} \left[1 + \nu \left(\hat{\mathbf{M}}_1 \hat{\mathbf{M}}_2(\lambda_F) \right)^2 \right]^{-2} \\ \times \left\{ \lambda \nu_1 \left[1 - \nu \left(\hat{\mathbf{M}}_1 \hat{\mathbf{M}}_2(\lambda_F) \right)^2 \right] \right. \\ \left. - 2b\nu \left(\hat{\mathbf{M}}_1 \hat{\mathbf{M}}_2(\lambda_F) \right) \right\}. \quad (27)$$

It is interesting to note that the general expression (25) for effective field is proportional to singular function $\delta(x - \lambda_F)$. It means the field vanishes everywhere except the SB layer near the interface $x = 0$ taken from the side of the layer **2**. Therefore the magnitude of the effective field is a bulk quantity depending on such bulk parameters as L, l_2, n_2, ν . But this field is applied near to interface only, namely, to the point $x = \lambda_F$.

This feature has a significant consequence. The action of the field may be described by two equivalent ways. One of them is to consider field (25) as a singular term in the bulk equations of motion LLG for the lattice magnetization. Exactly such a way was chosen in our previous preprint⁸ and article.⁷ But much more simple way is to include the field into the boundary condition for the lattice magnetization at the boundary point $x = \lambda_F$. This last way was proposed in Ref. 9 and we develop it here in the next section.

VI. BOUNDARY CONDITIONS FOR LATTICE MAGNETIZATION

We suggest a model, which is opposite to the model of uniformly spread spin transfer torque in the layer **2**. In our model, the spin transfer torque is localized inside the SB layer $0 < x < \lambda_F$ and may be described as a boundary condition. Such a model corresponds to the real situation if only the thickness of SB layer λ_F occurs the smallest length among the other lengths in the system (i.e., $L \gg \lambda_F, \sqrt{A} \gg \lambda_F$, and $l \gg \lambda_F$).

The total magnetization flux in the layers **1** and **3** consists only of mobile electron fluxes because magnetic lattice in the layer **1** is pinned, while the lattice in the layer **3** is nonmagnetic one. Therefore, fluxes in these layers may be described by means of expressions of the type (12). The situation with the layer **2** occurs significantly more complicated: mobile electrons and lattice both contribute to the flux. Mobile electrons contribute to longitudinal part of the flux, which coincides with Eq. (12), while the lattice creates a transverse part of the flux.

To derive all the spin fluxes, which may flow in our junction, it is convenient to return to initial equations (1)

and (5), sum them and rewrite in the form

$$\frac{\partial(\mathbf{M} + \mathbf{m})}{\partial t} + \gamma A \left[\mathbf{M}, \frac{\partial^2 \mathbf{M}}{\partial x^2} \right] + \gamma [\mathbf{M}, \mathbf{H}_{sd}] + \frac{\partial \mathbf{J}}{\partial x} \\ + \gamma [\mathbf{M}, \mathbf{H}'] + \gamma \alpha [\mathbf{m}, \mathbf{M}] - \frac{\kappa}{M} \left[\mathbf{M}, \frac{\partial \mathbf{M}}{\partial t} \right] \\ + \frac{\mathbf{m} - \bar{\mathbf{m}}}{\tau} = 0, \quad (28)$$

where $\mathbf{H}' = \mathbf{H} + \mathbf{H}_a + \mathbf{H}_d$. The summation of the initial Eqs. (1) and (5) is necessary to do in our case because the mobile electron flux may transfer to the lattice one and these fluxes together determine dynamics of the system. The second summand in the left hand side of Eq. (28) may be rewritten as follows:

$$\gamma A \left[\mathbf{M}, \frac{\partial^2 \mathbf{M}}{\partial x^2} \right] = a \frac{\partial}{\partial x} \left[\hat{\mathbf{M}}, \frac{\partial \mathbf{M}}{\partial x} \right] \equiv \frac{\partial \mathbf{J}_M}{\partial x}, \quad (29)$$

where

$$\mathbf{J}_M = a \left[\hat{\mathbf{M}}, \frac{\partial \mathbf{M}}{\partial x} \right] \quad (30)$$

may be considered as a lattice magnetization flux with parameter $a = \gamma AM$ having the sense of a lattice magnetization diffusion constant (see Refs. 7,8 for more details).

The next (third) summand in Eq. (28) may be transformed using formula (25) for \mathbf{H}_{sd} to the following form:

$$\gamma [\mathbf{M}, \mathbf{H}_{sd}] = \frac{\partial \mathbf{J}_{sd}}{\partial x}, \quad (31)$$

where

$$\mathbf{J}_{sd}(x) = \gamma h_{sd} l_2 \left[\mathbf{M}_2(\lambda_F), \hat{\mathbf{M}}_1 \right] \theta(x - \lambda_F) \quad (32)$$

represents a very interesting new quantity that may be called as an ‘‘effective field transverse flux’’ and $\theta(x - \lambda_F)$ is a well known step function: $\theta(x - \lambda_F) = 0$ for $x < \lambda_F$ and $\theta(x - \lambda_F) = 1$ for $x > \lambda_F$. Therefore, two lattice magnetization fluxes exist: (30) and (32), the last appearing due to sd effective field. All the lattice fluxes are perpendicular to the vector \mathbf{M}_2 . The fourth summand in Eq. (28) originates from mobile electron spin flux \mathbf{J} , which is given by Eq. (12). As it is seen, the flux \mathbf{J} is directed along vector \mathbf{M} .

Let us introduce the integration over the near-interface regions $-\lambda_F < x < -\varepsilon$ and $\varepsilon < x < \lambda_F$ with infinitesimal parameter $\varepsilon \rightarrow +0$ (see Fig. 2 for illustration):

$$\langle \dots \rangle_- \equiv \int_{-\lambda_F}^{-\varepsilon} (\dots) dx \quad \text{and} \quad \langle \dots \rangle_+ \equiv \int_{\varepsilon}^{\lambda_F} (\dots) dx \quad (33)$$

and apply these operations to Eq. (28). We should now introduce the conditions, which say explicitly that our nonmagnetic spacer layer appears nontransparent for the

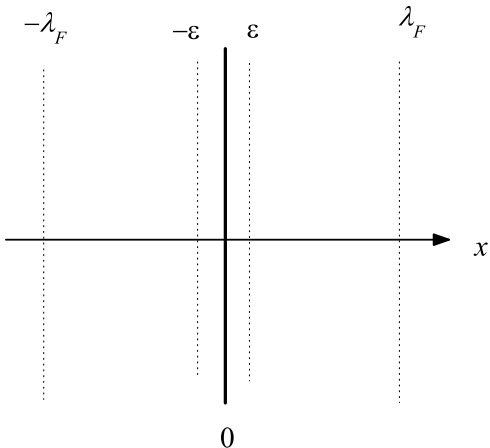


FIG. 2: Range of integration (33): the vertical dotted lines show limits of integration.

lattice magnetization excitations and fluxes. These conditions may be written as

$$\mathbf{J}_M(-\varepsilon) = 0, \quad \mathbf{J}_M(\varepsilon) = 0, \quad \mathbf{J}_{sd}(\varepsilon) = 0, \quad (34)$$

the latter condition being satisfied automatically because of the definition (32). Moreover, we accept the condition that our spacer is completely transparent for mobile electron spin flux that is no spin scattering processes occurs inside. This last condition may be written as

$$\mathbf{J}(-\varepsilon) = \mathbf{J}(\varepsilon). \quad (35)$$

After the operations (33) are applied, a number of simplifications become possible. In particular, two last summands in the left hand side of Eq. (28) may be considered as a very small in comparison with the first summand (since $0 < \kappa \ll 1$, $\omega\tau \ll 1$). These relaxation summands should be omitted if we want the flux continuity equations may be valid approximately. Further, there exist a number of “volume” summands, which are proportional to the small length λ_F . It is desirable these summands to be sufficiently small too, namely,

$$\lambda_F \left| \frac{\partial(\mathbf{M} + \mathbf{m})}{\partial t} + \gamma[\mathbf{M}, \mathbf{H}'] + \gamma\alpha[\mathbf{m}, \mathbf{M}] \right|_{-\lambda_F < x < -\varepsilon} \ll |\mathbf{J}(-\lambda_F)|, \quad (36)$$

$$\lambda_F \left| \frac{\partial(\mathbf{M} + \mathbf{m})}{\partial t} + \gamma[\mathbf{M}, \mathbf{H}'] + \gamma\alpha[\mathbf{m}, \mathbf{M}] \right|_{\varepsilon < x < \lambda_F} \ll |\mathbf{J}(\lambda_F) + \mathbf{J}_{sd}(\lambda_F)|. \quad (37)$$

The conditions (36) and (37) characterize an applicability of our model: the better they are satisfied, the more

exact is the model. Formally, conditions (36) and (37) are satisfied well in the limit $\lambda_F \rightarrow 0$.

Then, we apply (33) to (28) using Eqs. (34), (35) and making all the simplifications. We obtain as a result

$$-\mathbf{J}_M(-\lambda_F) - \mathbf{J}(-\lambda_F) + \mathbf{J}(\varepsilon) = 0, \quad (38)$$

$$\mathbf{J}(\lambda_F) - \mathbf{J}(\varepsilon) + \mathbf{J}_M(\lambda_F) + \mathbf{J}_{sd}(\lambda_F) = 0. \quad (39)$$

We put $\mathbf{J}_M(-\lambda_F) = 0$ in Eq. (38) because of \mathbf{M}_1 magnetization is pinned and, as we assume, cannot be excited by the electric current. The conditions (38) and (39) are valid for all the fluxes at the interface $x = 0$. Analogously, we may derive the conditions for the second interface $x = L$. The result is

$$\mathbf{J}(L + \varepsilon) - \mathbf{J}(L - \varepsilon) - \mathbf{J}_M(L - \varepsilon) = 0, \quad (40)$$

where we take into account the flux \mathbf{J}_{sd} is constant at $x = L$ and therefore falls out from the continuity condition. The conditions (38)–(40) represent in the most general vector form the quest boundary conditions. They allow us further to find all the necessary solutions of our initial equations of motion (1) and (5).

In particular, we obtain immediately the longitudinal boundary conditions (15) and (16) from Eqs. (38)–(40). To show this for forward current $j/e > 0$ we should simply multiply scalar Eqs. (38)–(40) by $\hat{\mathbf{M}}_2$. For $j/e < 0$, we multiply Eq. (40) by $\hat{\mathbf{M}}_2$ and multiply Eqs. (38) and (40) by $\hat{\mathbf{M}}_1$. Note, after the multiplication the products appear $\mathbf{J}_M(\lambda_F)\hat{\mathbf{M}}_1 \sim \sin \chi$ and $\mathbf{J}_{sd}(\lambda_F)\hat{\mathbf{M}}_1 \sim \sin \chi$, which are small at $\chi \ll 1$ and at $|\pi - \chi| \ll 1$. We shall consider in this paper (see Section VIII) only small or close to π angles χ . It gives us the reason to neglect further the products indicated that are proportional to $\sin \chi$.

The next step is to extract transverse part of the condition (39). According to Eq. (38), this part for the forward current $j/e > 0$ is induced by the component

$$\mathbf{J}_\perp(\varepsilon) \equiv \left[\hat{\mathbf{M}}_2(\lambda_F), \left[\mathbf{J}(-\lambda_F), \hat{\mathbf{M}}_2(\lambda_F) \right] \right] \quad (41)$$

and leads to the relation

$$\mathbf{J}_\perp(\varepsilon) = \mathbf{J}_M(\lambda_F) + \mathbf{J}_{sd}(\lambda_F). \quad (42)$$

For backward current $j/e < 0$ the other electron flux, namely, $\mathbf{J}(\lambda_F)$, induces transverse (perpendicular to \mathbf{M}_1) component while the flux $\mathbf{J}(\varepsilon)$ appears purely longitudinal one being collinear with \mathbf{M}_1 . This interesting process goes due to current dependent sd exchange effective field $\Delta\mathbf{H}_{sd}$ (see Eq. (25)) produces strong and localized influence on \mathbf{M}_2 by virtue the LLG equation should be satisfied. The field $\Delta\mathbf{H}_{sd}$ is directed parallel to \mathbf{M}_1 and therefore any transverse component of the mobile electron magnetization $\Delta\mathbf{m}_2$ inside the SB layer will decay

and transfer to the lattice, the transformation being analogous, in principal, to TST idea of the Refs. 1,2. Therefore, we may write the following induced transverse component for backward current $j/e < 0$:

$$\mathbf{J}_\perp(\lambda_F) = \left[\hat{\mathbf{M}}_1, \left[\mathbf{J}(\lambda_F), \hat{\mathbf{M}}_1 \right] \right], \quad (43)$$

which leads from Eq. (39) to the relation

$$\mathbf{J}_\perp(\lambda_F) = -\mathbf{J}_M(\lambda_F) - \mathbf{J}_{sd}(\lambda_F). \quad (44)$$

Transverse part of condition (40) occurs the same for both forward and backward current directions, $j/e > 0$ and $j/e < 0$, namely

$$\mathbf{J}_M(L - \varepsilon) = 0. \quad (45)$$

Now, we will try to represent conditions (42) and (44) in the forms, which are more convenient for further calculations. Let us multiply Eqs. (42) and (44) by $\hat{\mathbf{M}}_2(\lambda_F)$ vectorially and use relations (30), (32), (41), (43) and (12). Then, we get for $j/e > 0$

$$\begin{aligned} \frac{\partial \hat{\mathbf{M}}_2}{\partial x} \Big|_{x=\lambda_F} &= k \cdot \left[\hat{\mathbf{M}}_1, \hat{\mathbf{M}}_2(\lambda_F) \right] \\ -p \cdot \left[\hat{\mathbf{M}}_2(\lambda_F), \left[\hat{\mathbf{M}}_1, \hat{\mathbf{M}}_2(\lambda_F) \right] \right], \end{aligned} \quad (46)$$

where two new parameters k and p appear, which are given by formulae

$$k = \frac{1}{aM_2} \left(\frac{\mu_B}{e} Q_1 j - \tilde{D}_1 \frac{\partial \Delta m_1}{\partial x} \Big|_{x=-\lambda_F} \right) \quad \text{for } j/e > 0, \quad (47)$$

$$k = \frac{1}{aM_2} \left(\frac{\mu_B}{e} Q_2 j - \tilde{D}_2 \frac{\partial \Delta m_2}{\partial x} \Big|_{x=\lambda_F} \right) \quad \text{for } j/e < 0 \quad (48)$$

and

$$p = \frac{l_2 h_{sd}}{AM_2}, \quad (49)$$

where h_{sd} should be taken from formula (26) for $j/e > 0$ and from (27) for $j/e < 0$.

Parameter k originates from the contribution of mobile electron spin fluxes $\mathbf{J}_{1\perp}(\varepsilon)$ (41) and $\mathbf{J}_\perp(\lambda_F)$ (43), and therefore it describes the spin transfer torque action. Parameter p originates from $\mathbf{J}_{sd}(\lambda_F)$ flux (32) and describes action of the spin injection effective field. Let us substitute the before found expression Δm_1 (see Eqs. (19)–(22)) for $j/e > 0$ into (47) and corresponding expression Δm_2 for $j/e < 0$ into (48) to simplify both the expressions for k . It gives the following formulae simplified for the thin layer **2** that is for $\lambda \ll 1$:

$$k = \frac{\mu_B Q_1 j}{eaM_2} \frac{\nu}{\nu + \left(\hat{\mathbf{M}}_1 \hat{\mathbf{M}}_2(\lambda_F) \right)^2} \quad \text{for } j/e > 0 \quad (50)$$

and

$$k = \frac{\mu_B Q_1 j}{eaM_2} \frac{\nu \left(\hat{\mathbf{M}}_1 \hat{\mathbf{M}}_2(\lambda_F) \right)^2}{1 + \nu \left(\hat{\mathbf{M}}_1 \hat{\mathbf{M}}_2(\lambda_F) \right)^2} \quad \text{for } j/e < 0. \quad (51)$$

It is interesting to return now to the case of completely pinned layer **1** (that is not only the lattice magnetization but mobile electron spins also are pinned). We see from the first expression (47) the effective diffusion coefficient should be taken as $\tilde{D}_1 \rightarrow 0$. Then it follows from the parameters ν_1 and ν definitions made after the formulae (20), (21) and (26): $\nu_1 \rightarrow \infty$, $\nu \equiv \nu_1 \nu_2 \rightarrow \infty$. Substituting these limiting values to expressions (50), (51) and to (26), (27) we obtain

$$k = \frac{\mu_B Q_1 j}{aM_2 e}, \quad p = \frac{\mu_B \gamma \alpha_2 Q_1 \tau_2 \lambda}{a\nu_2} \left| \frac{j}{e} \right| \quad (52)$$

for a completely pinned layer **1** and for any sign of the current j/e . Therefore, the sign of the parameter k does depend on the sign of the current whereas parameter p is positive at any sign of the current. We shall see a little later this feature conserves in general case of non-pinned mobile electron spins (see formulae (59) and (60)) and it plays significant role in determining the instability character.

It remains now to rewrite the boundary condition (45) for the second interface $x = L$ in a more explicit form. Using the definition (30) and the equality $\left(\hat{\mathbf{M}}_2 \cdot \partial \hat{\mathbf{M}}_2 / \partial x \right)_{x=L-\varepsilon} \equiv 0$, we find

$$\frac{\partial \hat{\mathbf{M}}_2}{\partial x} \Big|_{x=L-\varepsilon} = 0. \quad (53)$$

VII. STATIC STATES

We start now to find solutions of LLG equation (1) satisfying our boundary conditions (46) and (53). We confine ourselves further to the situation when the current density j is considered as a fixed parameter given by an external circuit (the so called ‘‘current controlled regime’’). Moreover, we assume an external field \mathbf{H} is applied along the positive direction of z axis (see Fig. 1), and the anisotropy field \mathbf{H}_a is parallel to that axis too (remember: $H < H_a \ll 4\pi M$). Then in absence of current, when there is no coupling between the layers in our model, the layer **2** magnetization $\hat{\mathbf{M}}_2$ is aligned along z axis. Remember the vectors $\hat{\mathbf{M}}_1$ and $\hat{\mathbf{z}}$ make, in general, an angle χ in the model. Therefore we may write: $\hat{\mathbf{M}}_1 = -\hat{\mathbf{y}} \sin \chi + \hat{\mathbf{z}} \cos \chi$, where $\hat{\mathbf{x}}$, $\hat{\mathbf{y}}$ and $\hat{\mathbf{z}}$ are basis vectors of our coordinate system. After the current is turned on, the direction of the vector $\hat{\mathbf{M}}_2$ may change. Our task now is to search the vector $\hat{\mathbf{M}}_2$ change due to the current.

First, consider the static states possible when the fluctuations are neglected but the current presents, $j/e \neq 0$. We denote the static state magnetization as $\hat{\mathbf{M}}_2$.

To find the magnetization we would solve the equation $[\hat{\mathbf{M}}_2, \mathbf{H}_{eff}] = 0$, which follows from Eq. (1). The last equation and the boundary conditions are essentially nonlinear and nonuniform. Therefore general problem appears rather complicated even for finding the static states.

Fortunately, there exists one simple situation, which is at the same time the most actual one, namely, the situation with the angle $\chi = 0$ or $\chi = \pi$. In the situation all the boundary conditions and the equation of motion for $\hat{\mathbf{M}}_2$ are satisfied for

$$\hat{M}_{2x} = \hat{M}_{2y} = 0, \quad \hat{M}_{2z} = \pm 1. \quad (54)$$

The solution written can be easy justified by substitution of (54) into the equation and boundary conditions. We consider further only these last indicated values of the angle χ and therefore investigate the stability only for the static states (54). For definiteness, we will consider only the angle $\chi = \pi$ and therefore have

$$\hat{\mathbf{M}}_1 = -\hat{\mathbf{z}}. \quad (55)$$

As it is seen from Eqs. (54) and (55), two situations are possible: either vectors $\hat{\mathbf{M}}_2$ and $\hat{\mathbf{M}}_1$ are parallel each other (**P** state) or they are antiparallel (**AP** state). We shall consider further the both possibilities.

VIII. FLUCTUATIONS. DISPERSION RELATION

Passing to consideration of fluctuations $\Delta\hat{\mathbf{M}}_2$, we introduce them by the following relation:

$$\hat{\mathbf{M}}_2 = \pm\hat{\mathbf{z}} + \Delta\hat{\mathbf{M}}_2, \quad (56)$$

where $\Delta\hat{\mathbf{M}}_2 \equiv |\Delta\hat{\mathbf{M}}_2| \ll 1$. We linearize the LLG equation with respect to $\Delta\hat{\mathbf{M}}_2$ and, according to (25), lay $\Delta\mathbf{H}_{sd} \equiv 0$ outside the SB layer, that is for $x > \lambda_F$. The demagnetization field takes the form $\mathbf{H}_d = -4\pi M_2 \Delta\hat{M}_{2x} \hat{\mathbf{x}}$. Then the equations for fluctuations $\Delta\hat{M}_{2x,y} \sim \exp(-i\omega t)$ reduce to

$$\begin{aligned} \frac{\partial^2 \Delta\hat{M}_{2x}}{\partial x^2} - \frac{\Omega_1}{a} \Delta\hat{M}_{2x} - \frac{i\omega \hat{M}_{2z}}{a} \Delta\hat{M}_{2y} &= 0, \\ \frac{\partial^2 \Delta\hat{M}_{2y}}{\partial x^2} - \frac{\Omega_2}{a} \Delta\hat{M}_{2y} + \frac{i\omega \hat{M}_{2z}}{a} \Delta\hat{M}_{2x} &= 0, \end{aligned} \quad (57)$$

where two characteristic frequencies are introduced:

$$\begin{aligned} \Omega_1 &= \gamma \left(H \hat{M}_{2z} + H_a + 4\pi M_2 \right) - i\kappa\omega, \\ \Omega_2 &= \gamma \left(H \hat{M}_{2z} + H_a \right) - i\kappa\omega. \end{aligned} \quad (58)$$

We need now to linearize boundary conditions and use them together with equations (57). Parameters k and p

(47)–(49) should be taken for the static state chosen in the linear approximation. It means we need to rewrite general expressions (49)–(51) in a more specific form, which appears valid for any sign of current:

$$k = \frac{\mu_B Q_1}{a M_2} \frac{\nu}{1 + \nu} \cdot \frac{j}{e}, \quad (59)$$

$$p = \frac{\mu_B \gamma \alpha_2 \tau_2 Q_1}{a} \frac{[\lambda \nu_1 (\nu - 1) - 2b \nu \hat{M}_{2z}]}{(1 + \nu)^2} \left| \frac{j}{e} \right|. \quad (60)$$

Linearized boundary conditions after the transformations mentioned acquire the following form:

$$\left. \frac{\partial \Delta\hat{M}_{2x}}{\partial x} \right|_{x=\lambda_F} = k \Delta\hat{M}_{2y}(\lambda_F) - p \hat{M}_{2z} \Delta\hat{M}_{2x}(\lambda_F), \quad (61)$$

$$\left. \frac{\partial \Delta\hat{M}_{2y}}{\partial x} \right|_{x=\lambda_F} = -k \Delta\hat{M}_{2x}(\lambda_F) - p \hat{M}_{2z} \Delta\hat{M}_{2y}(\lambda_F), \quad (62)$$

$$\left. \frac{\partial \Delta\hat{M}_{2x}}{\partial x} \right|_{x=L-\varepsilon} = \left. \frac{\partial \Delta\hat{M}_{2y}}{\partial x} \right|_{x=L-\varepsilon} = 0. \quad (63)$$

Let us substitute $\Delta\hat{M}_{2x,y} \sim \exp(iqx')$ into equations (57) and define $x' = x - \lambda_F$. Then we find four possible characteristic wave numbers:

$$q_{\pm}^2 = -\frac{1}{2a} \left[\Omega_1 + \Omega_2 \pm \sqrt{(\Omega_1 - \Omega_2)^2 + 4\omega^2} \right]. \quad (64)$$

Then, the general solution of our linearized equations (57) may be presented as follows

$$\begin{aligned} \Delta\hat{M}_{2x}(x') &= A \cos q_- x' + B \sin q_- x' \\ &\quad + C \cos q_+ x' + D \sin q_+ x', \\ \Delta\hat{M}_{2y}(x') &= \xi (A \cos q_- x' + B \sin q_- x') \\ &\quad + \xi^{-1} (C \cos q_+ x' + D \sin q_+ x'), \end{aligned} \quad (65)$$

where we took $\text{Re } q_{\pm} > 0$ and introduced a ‘‘distribution coefficient’’

$$\xi = 2i\omega \hat{M}_{2z} \left[\Omega_2 - \Omega_1 + \sqrt{(\Omega_1 - \Omega_2)^2 + 4\omega^2} \right]^{-1}. \quad (66)$$

Constants A, B, C, D should be found now from the boundary conditions (61)–(63). Substituting (66) into the conditions and equating the determinant to zero, we find the dispersion relation for the fluctuations in the most general form:

$$\begin{aligned} &\left(q_- \tan q_- L + p \hat{M}_{2z} \right) \left(q_+ \tan q_+ L + p \hat{M}_{2z} \right) \\ &+ k^2 + \frac{2\xi k}{1 - \xi^2} (q_- \tan q_- L - q_+ \tan q_+ L) = 0. \end{aligned} \quad (67)$$

We may compare Eq. (67) with before derived dispersion relation in Refs. 7,8. Note, parameter $\xi^2 \neq 1$. It

can be seen directly from the definitions (66) and (58). Taking this into account, we see the relations mentioned may be exactly reduced to each other but for the case $k = 0$ only, that is for the case of the LSI effective field mechanism is dominated. It appears due to rather crude approximation used in Refs. 7,8 when deriving the dispersion relation. Contrary to this, our last expression (67) represents more correct and complete dispersion relation, which describes joint action of TST torque and LSU effective field mechanisms.

IX. INSTABILITY OF FLUCTUATIONS

We need further to solve the dispersion relation (67) and find eigenfrequencies ω for fluctuations. In particular, it allows us to determine the current driven instability condition, that is the condition when $\text{Im} \omega > 0$. Generally speaking, the transcendental equation (67) may be solved numerically for a number of experimentally given junction parameters. However, the actual task now is to develop a general representation about the switching process rather than to get specific numerical results. To fulfil the task, we may try to solve the equation analytically but only for a special case of nearly uniform fluctuations which satisfy the equality $\tan q_- L \approx q_- L$.

It is convenient to use Eqs. (64), (66) and rewrite Eq. (67) in the form

$$\begin{aligned} & \Omega_1 + \Omega_2 - \sqrt{(\Omega_1 - \Omega_2)^2 + 4\omega^2} \\ &= \left(\frac{2a}{L}\right) \left[p\hat{M}_{2z} + \frac{k^2}{q_+ \tan q_+ L + p\hat{M}_{2z}} \right. \\ & \left. + \frac{2i\omega k \hat{M}_{2z}}{a(q_+^2 - q_-^2)} \left(1 - \frac{q_-^2 L + p\hat{M}_{2z}}{q_+ \tan q_+ L + p\hat{M}_{2z}} \right) \right]. \end{aligned} \quad (68)$$

If current is absent (that is $k = p = 0$), we obtain from Eq. (68)

$$\begin{aligned} \frac{\omega}{\omega_0} &= \sqrt{(1 + \kappa^2) \left(1 + \frac{h\hat{M}_{2z}}{h_a} \right) - \frac{\kappa^2}{4h_a} - i \frac{\kappa}{2\sqrt{h_a}}}, \\ \omega_0 &= \frac{4\pi\gamma M_2}{1 + \kappa^2} \sqrt{h_a}, \end{aligned} \quad (69)$$

where we remain only positive frequency $\text{Re} \omega \geq 0$ and introduced dimensionless fields: $h = H/4\pi M_2$ and $h_a = H_a/4\pi M_2$. According to typical values of parameters, we have $H \sim 10\text{--}100$ Oe, $H_a \sim 100$ Oe, $M_2 \sim 10^3$ G and therefore $h, h_a \lesssim 0.01$. We neglect small corrections originated due to higher powers of h, h_a in Eq. (69). As it is seen from Eq. (69), the fluctuations without current are, of course, stable due to the Gilbert damping.

Return now to the situation when the current is turned on ($j \neq 0$) but is not too large in magnitude to allow preserve in Eq. (68) only linear in current summands. The justification of the supposition will be considered later,

at the end of the section. If we accept now that the supposition is valid, it becomes possible to insert $q_- = 0$ into the square brackets of Eq. (68). It means, in particular, we may lay $\sqrt{(\Omega_1 - \Omega_2)^2 + 4\omega^2} = \Omega_1 + \Omega_2$ in the definition (64) of q_+ and therefore use the expression

$$q_+ \approx i\sqrt{\frac{\Omega_1 + \Omega_2}{a}} \quad (70)$$

to substitute it to the right hand side of Eq. (68). Moreover, we should neglect summands proportional to k^2 and kp too. Formally, these simplifications become valid if the following conditions are fulfilled:

$$\frac{a|p|}{L|\Omega_1 + \Omega_2|} \ll 1, \quad \left| \frac{k^2}{pq_+} \right| \ll 1, \quad \left| \frac{p}{q_+} \right| \ll 1. \quad (71)$$

Then we resolve Eq. (68) with respect to square root and square the result. Some summands appear containing second (or higher) power of the current (k^2, kp and so on). These summands are small also and should be neglected due to the conditions (71). After we make the simplifications and substitute (70), we obtain the following square equation for the eigenfrequency ω :

$$\begin{aligned} & \omega^2(1 + \kappa^2) + i\kappa\omega \left[\text{Re}(\Omega_1 + \Omega_2) - \frac{2ap\hat{M}_{2z}}{L} - \frac{2ak\hat{M}_{2z}}{\kappa L} \right] \\ & - \left[\text{Re}(\Omega_1\Omega_2) - \frac{ap\hat{M}_{2z}}{L} \text{Re}(\Omega_1 + \Omega_2) \right] = 0. \end{aligned} \quad (72)$$

We should solve the equation (72) using the definitions of the parameters k and p given by Eqs. (59) and (60). Then we obtain finally

$$\begin{aligned} \frac{\omega}{\omega_0} &= -i \frac{\kappa_0}{2\sqrt{h_a}} \left[\frac{\kappa}{\kappa_0} - \frac{\hat{M}_{2z}(j/e)}{(j_0/|e|)} \right] \\ & + \left\{ (1 + \kappa^2) \left(1 + \frac{\hat{M}_{2z}h}{h_a} - \frac{\hat{M}_{2z}|j|}{j_0} \right) \right. \\ & \left. - \left(\frac{\kappa_0}{2\sqrt{h_a}} \right)^2 \left[\frac{\kappa}{\kappa_0} - \frac{\hat{M}_{2z}(j/e)}{(j_0/|e|)} \right]^2 \right\}^{1/2}, \end{aligned} \quad (73)$$

where we used the following simplifying assumption

$$\eta \equiv \frac{|k|}{\kappa|p|} \gg 1, \quad (74)$$

which is really true for many actual cases of small enough Gilbert parameter κ . Formula (73) reduces to (69) in the limit $j \rightarrow 0$. The following additional system characteristics are introduced in Eq. (73):

characteristic damping

$$\kappa_0 = \frac{2h_a\nu(\nu + 1)}{\gamma\alpha_2\tau_2 M_2 \left[\lambda\nu_1(\nu - 1) - 2b\nu\hat{M}_{2z} \right]} \quad (75)$$

and

characteristic current density

$$(j_0/|e|) = \frac{4\pi M_2 l_2 h_a \lambda (\nu + 1)^2}{\mu_B \alpha_2 \tau_2 Q_1 \left[\lambda \nu_1 (\nu - 1) - 2b\nu \hat{M}_{2z} \right]}. \quad (76)$$

Here the matching parameters ν_1 and ν are exactly the same as they were defined after formulae (20), (21) and (26). We may substitute the following typical values: $\nu_2 \sim 1$, $\nu_1 \gg 1$ and $\nu \gg 1$, $\lambda \sim 0.1$, $l \sim 17$ nm, $\alpha_2 \sim 2 \times 10^4$, $\tau_2 \sim 3 \times 10^{-13}$ s, $Q_1 \sim Q_2 \sim 0.3$. Then we get the estimations: $|\kappa_0| \sim 3 \times 10^{-2}$, $|j_0| \sim 1 \times 10^7$ A/cm².

Expression (73) allows write the following two conditions of instability ($\text{Im } \omega > 0$):

$$\hat{M}_{2z} \frac{|j|}{j_0} > 1 + \frac{\hat{M}_{2z} h}{h_a}, \quad (77)$$

$$\hat{M}_{2z} \frac{j/e}{j_0/|e|} > \frac{\kappa}{\kappa_0}. \quad (78)$$

The fulfillment of any of the conditions (77) or (78) or both of them together is sufficient for instability. The condition (77) originates from p parameter and therefore refers to LSI mechanism. The condition (78) originates from k parameter and refers to TST mechanism. The threshold current j_{th} has a minimal module, which is necessary to reach the instability according to Eqs. (77) and (78), that is

$$j_{th} = |j_0| \cdot \min \left(\left| 1 + \frac{\hat{M}_{2z} h}{h_a} \right|, \frac{\kappa}{|\kappa_0|} \right). \quad (79)$$

As it is seen, the threshold for LSI mechanism does not depend on the Gilbert constant κ , while the TST threshold is directly proportional to it. Because of experimentally revealed damping at room temperature³³ $\kappa \approx (2 \div 5) \times 10^{-2}$ corresponds to the above given estimation $\kappa \sim |\kappa_0| \sim 3 \times 10^{-2}$, we may expect any of the mechanism, in principle, is responsible for the instability. Note, the parameters j_0 and κ_0 , according to the definitions (75) and (76), may change their signs and become negative. But it may occur only simultaneously for j_0 and κ_0 . Therefore, the TST condition (78) does not depend on the sign at all, but to provide the LSI instability condition be fulfilled we should change the sign of \hat{M}_{2z} only.

Let us take for further estimations:

$$\left| 1 + \frac{\hat{M}_{2z} h}{h_a} \right| \sim 1 \quad \frac{\kappa}{|\kappa_0|} \leq 1 \quad \text{or} \quad \frac{\kappa}{|\kappa_0|} \sim 1 \quad (80)$$

and moreover $\nu \gg 1$, $\nu_2 \sim 1$ and all the estimations from the text are valid. Then, we substitute these parameters into conditions (71) and get

$$\frac{a|p|}{L|\Omega_1 + \Omega_2|} \sim 10^{-2}, \quad \left| \frac{k^2}{pq_+} \right| \sim 10^{-4}, \quad \left| \frac{p}{q_+} \right| \sim 10^{-2}.$$

We see, therefore, the conditions (71) are good satisfied for the threshold current and even above it. The last estimations justify our above-stated analytic approach to the solution of the dispersion relation (67). It is interesting to stress, our eigenfrequency ω (73) appears essentially nonlinear function of the current j/j_0 in spite of the linearization conditions (71).

X. STATE DIAGRAM AND HYSTERESIS

We discuss now in detail the instability conditions (77) and (78). Let us draw the corresponding threshold curves in the current to damping plane — the “state diagram”. The result is presented qualitatively in Fig. 3. We confined ourselves only the case of positive parameters $j_0 > 0$ and $\kappa_0 > 0$ and built up the boundaries of the regions indicated. The condition (77) can be satisfied for $\hat{M}_{2z} = 1$ only. It means the LSI mechanism can excite the instability of **AP** state only to switch it into **P** state. That is true whatever sign is taken for the current. Another situation appears in connection with the condition (78). For forward current $j/e > 0$ the only value $\hat{M}_{2z} = 1$ is acceptable, but for backward current $j/e < 0$ it is necessary to have $\hat{M}_{2z} = -1$. It means the TST mechanism excites the instability of different states depending on the sign of the current: forward current excites **AP** state, but backward current excites **P** state. All these possibilities are seen from Fig. 3.

Two notes should be made here. First, let us go along the line $o_1 a$ having **AP** state. In the point a the state becomes unstable and will be switched to the stable **P** state. We may return then to the point b , where the **P** state becomes unstable and will be switched to the initial **AP** state, which now is stable, and so on. Any switching process leads to change of the junction resistance, the higher resistance being correspond to **AP** state and the lower resistance to **P** state. Such a behavior is illustrated in Fig. 4 and similar observations were revealed experimentally in many papers.

The second note concerns the intersections of our line $o_1 a$ in Fig. 3 or some other lines ($o_2 c$, for example) with the threshold curves in the points b' , d' and so on. In the points all the initial states, **AP** and **P**, become unstable. Therefore, no switching can appear and instead some new time dependent oscillatory state, apparently, should form. This is a very interesting possibility, which correlates with the well known experimental observations of a microwave emission from the junctions above the instability threshold (see, e.g., Ref. 12). We plan to investigate the possibility in more detail elsewhere.

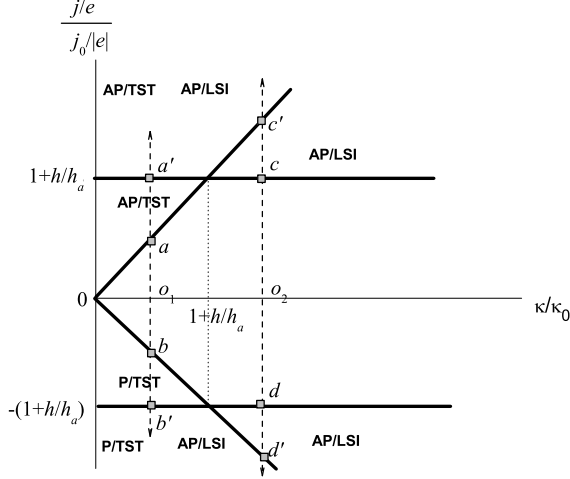


FIG. 3: State diagram. Threshold current versus damping (qualitatively) at $\nu_1(\nu - 1)\lambda \gg 2b\nu$, $\nu_1 \gg 1$, $\nu_2 = 1$. Heavy lines show boundaries of the regions. The following notations are introduced: **AP/LSI** means that **AP** initial state is unstable due to LSI mechanism; **P/TST** means that **P** initial state is unstable due to TST mechanism, and so on. The region around the line $j = 0$ without any designations corresponds to stability. Points of switching: a — switching **AP** \rightarrow **P**, b — switching **P** \rightarrow **AP**, c and d — switching **AP** \rightarrow **P**. Points of oscillations: b' and d' .

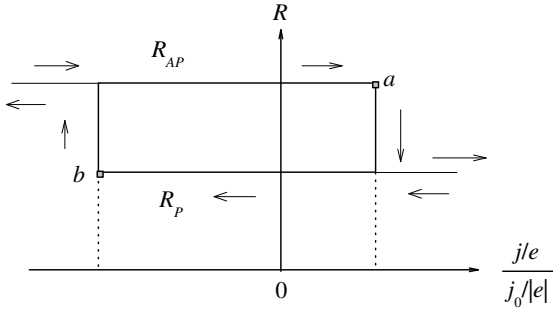


FIG. 4: Hysteretic behavior of junction resistance R : R_{AP} , R_P are resistances of **AP** and **P** states, respectively.

XI. SPECTRUM SOFTENING AND INCREMENT

We discuss now the question: how spectrum ($\text{Re}\omega$) and increment ($\text{Im}\omega$) behave when the current comes near the threshold of instability. To answer, we consider Eq. (73) for eigenfrequency and calculate numerically the quantities of interest for some typical example. Figs. 5–7 demonstrate the most significant results.

According to Fig. 5, a normalized spectrum $\text{Re}\omega/\omega_0$

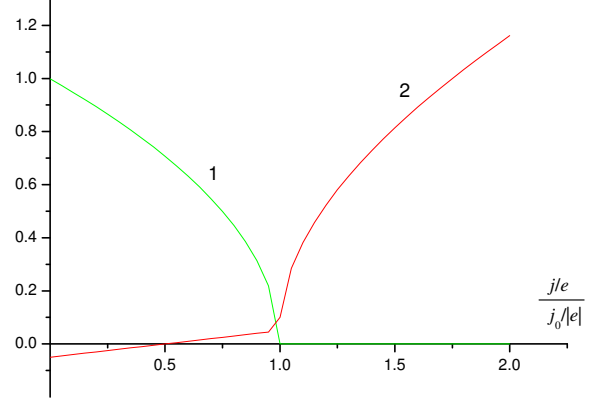


FIG. 5: (Color online) Current dependence of eigenfrequency $\text{Re}\omega/\omega_0$ (curve 1) and decrement $\text{Im}\omega/\omega_0$ (curve 2). Damping constant $\kappa/\kappa_0 = 0.5$.

falls to zero, that is softens, when the current rises nearing to the LSI threshold. As it was remarked in Ref. 7, the softening appears due to LSI driven reorientation phase transition at the threshold. Indeed, such a softening is the general property of similar phase transitions. Contrary to this, the TST has no relation to any phase transition⁷ and is simply a mechanism to deliver energy into the magnetic lattice. correspondingly, increment $\text{Im}\omega/\omega_0$ changes its sign and becomes positive not at the LSI threshold but a little below if damping is small enough, namely, for $\kappa/\kappa_0 = 0.5$ in our example. It is significant to stress the increment rises faster when current increases in the region where the LSI mechanism dominates. If we estimate $\omega_0 \sim 10^{10} \text{ s}^{-1}$, then the increment may rise from approximately $\text{Im}\omega \sim 10^9 \text{ s}^{-1}$ for TST mechanism dominated to $\text{Im}\omega \sim 10^{10} \text{ s}^{-1}$ for LSI mechanism dominated.

Fig. 6 shows the spectrum for different values of an external magnetic field. Eigenfrequencies rise with increasing the field. The LSI threshold shifts toward large currents. But the fact of spectrum softening, of course, remains.

Fig. 7 shows the increment for different values of a damping constant and in absence of external magnetic field. As the damping increases, the increment at a given current decreases for any mechanisms (TST and LSI) but LSI threshold is fixed, that is it does not depend on the damping. The TST threshold rises with damping and reaches the LSI threshold at the end.

XII. CONCLUSION

A phenomenological approach is developed in the theory of spin-valve type ferromagnetic junctions. New vector boundary conditions are derived, which represent the

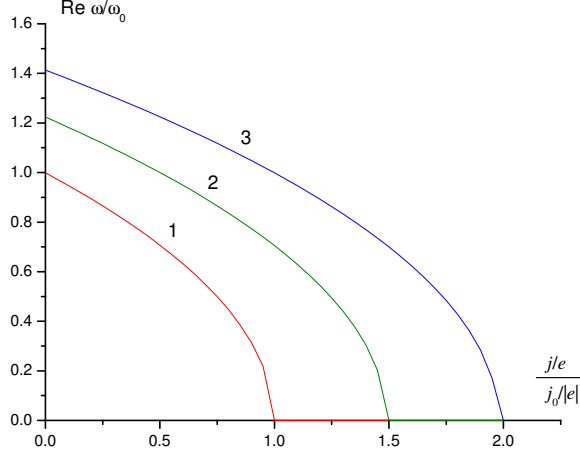


FIG. 6: (Color online) Softening of eigenfrequency for different external fields: 1 — $h/h_a = 0$, 2 — $h/h_a = 0.5$, 3 — $h/h_a = 1.0$. Parameters: $\nu \gg 1$, $b \sim 1$, $\kappa_0/(2\sqrt{h_a}) = 0.1$.

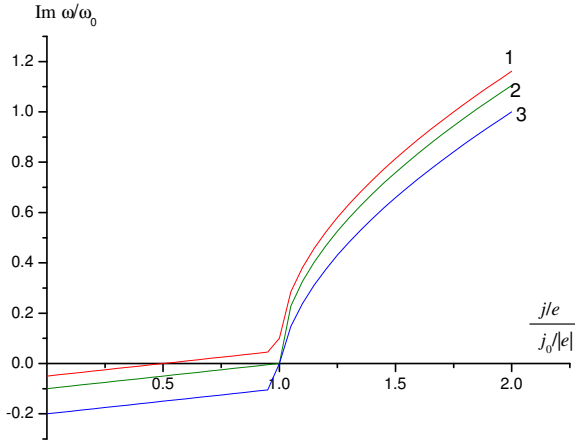


FIG. 7: (Color online) Increments for different damping: 1 — $\kappa/\kappa_0 = 0.5$, 2 — $\kappa/\kappa_0 = 1.0$, 3 — $\kappa/\kappa_0 = 2.0$. Parameters: $\nu \gg 1$, $b \sim 1$, $h = 0$, $\kappa_0/(2\sqrt{h_a}) = 0.1$.

continuity conditions for different spin fluxes: longitudinal spin flux of mobile electrons and transverse spin fluxes of the magnetic lattice including the so called “effective field transverse spin flux”. Spin transfer torque is considered as a boundary condition. It describes the result of abrupt transformation of the mobile electron transverse spin flux to the spin fluxes of the lattice. Joint action of two electric current effects is investigated: the nonequilibrium longitudinal spin injection effective field and the transverse spin transfer surface torque. General macroscopic dynamic equations are linearized for fluctuations and solved using the boundary conditions mentioned. Dispersion relation is derived and solved.

The calculation model is extended significantly to make it adequate the experimental situation as far as it is possible. In particular, the mobile electrons are considered as having non-pinned spins in all the contacting layers. Lattice magnetization is assumed completely pinned in one of the magnetic layers and free in the other magnetic layer. Theory is developed for any current direction in the spin-valve junction (forward or backward).

Some critical value κ_0 of the well known Gilbert damping constant κ is introduced for the first time. Spin transfer torque gives the dominant contribution to instability threshold for small enough constants $\kappa < \kappa_0$, while the spin injection contribution dominates for $\kappa > \kappa_0$. Typical estimation gives $\kappa_0 \sim 3 \times 10^{-2}$ and it approximately corresponds to the experimentally found Gilbert constant values for ferromagnetic metals at room temperature. It means both the two mechanisms may be responsible for the measured thresholds.

The mechanism of magnetic switching by the backward current and hysteretic behavior is proposed for the first time. As it appears, a fine interplay of spin transfer torque and spin injection is necessary to provide the hysteresis. The peculiarity of the process may be understood as follows. Spin injection effective field is localized in the free layer near the boundary between pinned and free layers. Spins of mobile electrons in the backward current have a component transverse to the effective field and therefore perform a precession in the field. This precession leads to torque generation and switching in complete accordance with the transverse spin transfer mechanism. The consequent realization of forward and such type of backward switching leads to hysteretic behavior shown in Fig. 4. The existence of the hysteresis is consistent with experimental data.

The state diagram was built up that divided the current–damping plane (Fig. 3) into regions of fluctuation stability and regions of various type instabilities. For example, for forward currents the **AP** initial states may become unstable and **P** states remain stable. In the regions the switching processes (i.e., **AP** → **P**) become possible. This diagram revealed for the first time the existence of another type regions for backward currents where **AP** and **P** initial states become unstable simultaneously. This last type of regions may correspond to formation of time dependent (oscillatory) states as a result of the instability development.

The effect of softening was predicted for the layer spin wave eigenfrequencies when current rises and comes to the instability threshold (Figs. 5 and 6). This effect is interesting because it distinguishes directly between TST and LSI mechanisms, since only the LSI mechanism leads to the softening.

The estimations were made of instability increments as functions of the current. It was shown for the first time that LSI mechanism leads to much larger increments in comparison with TST mechanism. For example, if we take spin wave eigenfrequency $\text{Re } \omega \sim 10^{10} \text{ s}^{-1}$, then we get increment $\text{Im } \omega \sim 10^9 \text{ s}^{-1}$ for TST mechanism dom-

inated and $\text{Im}\omega \sim 10^{10} \text{ s}^{-1}$ for LSI mechanism dominated. The increment rises for any mechanism if current increases and damping decreases.

Acknowledgments

The authors are thankful to Professor Sir Roger Elliott for attraction of their attention to the problem of ferromagnetic junction switching and for fruitful collaboration.

The work was supported by Russian Foundation for Basic Research, Grant No. 06-02-16197.

APPENDIX: TRANSVERSE SPIN TRANSFER TORQUE CONSIDERED AS A LOCALIZED OR AS A UNIFORMLY SPREAD

We try now to show the connections between two models discussed till now: traditional model of uniformly spread TST torque and recently introduced (Refs. 7,8, 9,10 and this paper) localized TST torque.

We start from the linearized equations and boundary conditions for fluctuations (57) and (61)–(63). The boundary conditions (61) and (62) may be inserted into Eq. (57) using a singular δ -function, namely,

$$\begin{aligned} & \frac{\partial^2 \Delta \hat{M}_{2x}}{\partial x^2} - \frac{\Omega_1}{a} \Delta \hat{M}_{2x} - \frac{i\omega \hat{M}_{2z}}{a} \Delta \hat{M}_{2y} \\ &= \left[k \Delta \hat{M}_{2y} - p \hat{M}_{2z} \Delta \hat{M}_{2x} \right] \delta(x - \lambda_F), \\ & \frac{\partial^2 \Delta \hat{M}_{2y}}{\partial x^2} - \frac{\Omega_2}{a} \Delta \hat{M}_{2y} + \frac{i\omega \hat{M}_{2z}}{a} \Delta \hat{M}_{2x} \\ &= \left[-k \Delta \hat{M}_{2x} - p \hat{M}_{2z} \Delta \hat{M}_{2y} \right] \delta(x - \lambda_F). \end{aligned} \quad (\text{A.1})$$

To check the correspondence of the Eqs. (A.1) and (57), (61), (62), let us integrate (A.1) over the interval $[0, \lambda_F + 0]$. Then, we have for the derivative

$$\begin{aligned} \int_0^{\lambda_F} \frac{\partial^2 \Delta \hat{M}_{2x}}{\partial x^2} dx &= \left[\frac{\partial \Delta \hat{M}_{2x}}{\partial x} \Big|_{x=\lambda_F} - \frac{\partial \Delta \hat{M}_{2x}}{\partial x} \Big|_{x=0} \right] \\ &= \frac{\partial \Delta \hat{M}_{2x}}{\partial x} \Big|_{x=\lambda_F} \end{aligned} \quad (\text{A.2})$$

and analogous expression for the other derivative, which may be got by a replacement $x \rightarrow y$, where we accept free spins at the plane $x = 0$, that is

$$\frac{\partial \Delta \hat{M}_{2x}}{\partial x} \Big|_{x=0} = \frac{\partial \Delta \hat{M}_{2y}}{\partial x} \Big|_{x=0} = 0. \quad (\text{A.3})$$

Moreover, we should neglect all the terms, which are proportional to small length $\lambda_F \rightarrow 0$. Then we get immediately the boundary conditions in the form (61), (62).

Therefore, two completely equivalent approaches may be used: either we solve our previous equations (57) satisfying nonuniform system of boundary conditions (61)–(63), or we solve the singular equations (A.1) with uniform boundary conditions (63) and (A.3).

The second approach appears convenient to pass to uniform model. To do this, we should spread uniformly through the whole layer **2** thickness L the localized excitation in (A.1), that is we should take

$$\delta(x - \lambda_F) \rightarrow \frac{1}{L}. \quad (\text{A.4})$$

After this is done, the equations (A.1) become spatially uniform and exactly coincide with the linearized uniform model. The last statement may be directly confirmed if we start from LLG equation with the well known additional double vector product term introduced in the original works^{1,2}. The boundary conditions (63) and (A.3) are uniform also. It shows we can find a uniform solution for fluctuations. To simplify extremely the calculations, we suppose the thickness of the layer is sufficiently small and spin injection may be omitted. Then the following dispersion relation for eigenfrequency becomes valid in linear in current approximation:

$$\begin{aligned} (1 + \kappa^2)\omega^2 + i\kappa\omega \left[\text{Re}(\Omega_1 + \Omega_2) - \frac{2ak}{\kappa L} \hat{M}_{2z} \right] \\ - \text{Re}(\Omega_1 \Omega_2) = 0. \end{aligned} \quad (\text{A.5})$$

This dispersion relation coincides with the corresponding relation of our localized torque model (72) taken at $p = 0$. The condition of instability that follows from (A.5) may be written in the form

$$\hat{M}_{2z} \cdot \frac{j_{th,\perp}}{e} > \frac{2\pi\gamma M_2^2 \kappa L (1 + \nu)}{\mu_B \nu Q_1}. \quad (\text{A.6})$$

As it is seen, forward current ($j_{th,\perp}/e > 0$) leads to instability of **AP** states only (because of to satisfy (A.6) we should take $\hat{M}_{2z} = 1$) and, vice versa, backward current ($j_{th,\perp}/e < 0$) leads to instability of **P** states (we should take $\hat{M}_{2z} = -1$). This conclusion is in agreement with our localized torque theory (see Section X of this paper). Numerical estimation gives $|j_{th,\perp}/e| \sim 10^7 \text{ A/cm}^2$.

However, we should stress here the correct understanding of the problem cannot be possible without including both the mechanisms (TST and LSI) acting simultaneously. First, the LSI was included implicitly in the condition (A.6) for backward current switching. Really, the existence of *sd* exchange effective field $\Delta \mathbf{H}_{sd} \sim \delta(x - \lambda_F)$ (see Eq. (25)) is necessary to understand the backward transverse spin flux appearing in the layer **2** and transformation of this flux into the lattice flux. The relation (44) describes such a transformation and allows calculate the TST parameter k (52).

Moreover, the results of the paper show the LSI mechanism manifests itself significantly and in different ways. For example, the instability threshold does not rise with

increasing the Gilbert damping constant κ but reaches some limiting value due to LSI mechanism (see Fig. 3). Increment of instability may be more than order of magnitude larger due to LSI (see Fig. 5). Interplay of TST and LSI mechanisms makes it possible to provide the in-

stability simultaneously of \mathbf{P} and \mathbf{AP} states (Fig. 3). It means, no switching but rather new time dependent final nonlinear state may appear as a result of the instability development.

* Electronic address: zil@ms.ire.rssi.ru

- ¹ J. C. Slonczewski, J. Magn. Magn. Mater. **159**, L1 (1996).
- ² L. Berger, Phys. Rev. B **54**, 9353 (1996).
- ³ C. Heide, P. E. Zilberman, and R. J. Elliott, Phys. Rev. B **63**, 064424 (2001).
- ⁴ Yu. V. Gulyaev, P. E. Zilberman, E. M. Epshtein, and R. J. Elliott, JETP Lett. **76**, 155 (2002).
- ⁵ R. J. Elliott, E. M. Epshtein, Yu. V. Gulyaev, and P. E. Zilberman, J. Magn. Magn. Mater. **271**, 88 (2004).
- ⁶ Yu. V. Gulyaev, P. E. Zilberman, E. M. Epshtein, and R. J. Elliott, JETP Lett. **79**, 402 (2004).
- ⁷ Yu. V. Gulyaev, P. E. Zilberman, E. M. Epshtein, and R. J. Elliott, JETP **127**, 1005 (2005).
- ⁸ R. J. Elliott, E. M. Epshtein, Yu. V. Gulyaev, and P. E. Zilberman, cond-mat/0412523.
- ⁹ R. J. Elliott, E. M. Epshtein, Yu. V. Gulyaev, and P. E. Zilberman, cond-mat/0505268.
- ¹⁰ R. J. Elliott, E. M. Epshtein, Yu. V. Gulyaev, and P. E. Zilberman, J. Magn. Magn. Mater. **300**, 122 (2006).
- ¹¹ E. B. Myers, D. C. Ralph, J. A. Katine, R. N. Louie, and R. A. Buhrman, Science **285**, 867 (1999).
- ¹² M. Tsoi, A. G. M. Jansen, J. Bass, W. C. Chiang, M. Seck, V. Tsoi, and P. Wyder, Phys. Rev. Lett. **80**, 4281 (1998); **81**, 493 (E) (1998).
- ¹³ F. J. Albert, N. C. Emley, E. B. Myers, D. C. Ralph, and R. A. Buhrman, Phys. Rev. Lett. **89**, 226802 (2002).
- ¹⁴ J.-E. Wegrowe, Phys. Rev. B **68**, 214414 (2003).
- ¹⁵ J. Grollier, V. Cross, H. Jaffres, A. Hamzic, J. M. George, G. Faini, J. Ben Youssef, H. Le Gall, and A. Fert, Phys. Rev. B **67**, 174402 (2003).
- ¹⁶ T. Y. Chen, Y. Ji, and C. L. Chien, Appl. Phys. Lett. **84**, 380 (2004).
- ¹⁷ Y. Huai, F. Albert, P. Nguyen, M. Pakala, and T. Valet, Appl. Phys. Lett. **84**, 3118 (2004).
- ¹⁸ I. N. Krivorotov, N. C. Emley, J. C. Sankey, S. I. Kiselev, D. C. Ralph, and R. A. Buhrman, Science **307**, 228 (2005).
- ¹⁹ M. D. Stiles and A. Zangwill, Phys. Rev. B **66**, 014407 (2002).
- ²⁰ M. D. Stiles, J. Xiao, and A. Zangwill, Phys. Rev. B **69**, 054408 (2004).
- ²¹ D. M. Edwards and F. Federici, cond-mat/0506086.
- ²² D. M. Edwards, F. Federici, J. Mathon, and A. Umerski, Phys. Rev. B **71**, 054407 (2005).
- ²³ S. Zhang, P. M. Levy, and A. Fert, Phys. Rev. Lett. **88**, 236601 (2002).
- ²⁴ A. Rebei, W. N. G. Hitchon, and G. J. Parker, Phys. Rev. B **72**, 064408 (2005).
- ²⁵ J. Grollier, V. Cross, A. Hamzic, J. M. George, H. Jaffres, A. Fert, G. Faini, J. Ben Youssef, and H. Legall, Appl. Phys. Lett. **78**, 3663 (2001).
- ²⁶ A. N. Slavin and P. Kabos, IEEE Trans. on Magnetics **41**, 1264 (2005).
- ²⁷ E. L. Nagaev, *Physics of Magnetic Semiconductors* (Moscow, Mir Publishers, 1983).
- ²⁸ A. I. Akhiezer, V. G. Baryakhtar, and S. V. Peletminskii, *Spin Waves* (Amsterdam, North-Holland Publ. Co., 1968).
- ²⁹ T. Valet and A. Fert, Phys. Rev. B **48**, 7099 (1993).
- ³⁰ A. K. Zvezdin and K. A. Zvezdin, Bulletin of the Lebedev Physics Institute No. 8, 3 (2002).
- ³¹ Yu. V. Gulyaev, P. E. Zilberman, and E. M. Epshtein, J. Commun. Technol. and Electronics **48**, 942 (2003).
- ³² A. Fert and H. Jaffres, Phys. Rev. B **64**, 184420 (2001).
- ³³ S. Ingvarsson, L. Ritchie, X. Y. Liu, Gang Xiao, J. C. Slonczewski, P. L. Trouilloud, and R. H. Koch, Phys. Rev. B **66**, 214416 (2002).
- ³⁴ B. P. Zakharchenya, D. N. Mirlin, V. I. Perel, and I. I. Reshina, Sov. Phys. Usp. **25**, 143 (1982).
- ³⁵ A. G. Aronov, JETP Lett. **24**, 32 (1976).
- ³⁶ A. G. Aronov and G. E. Pikus, Sov. Phys. Semicond. **10**, 698 (1976).
- ³⁷ W. Shockley, *Electrons and Holes in Semiconductors, with Applications to Transistor Electronics*, (New York, Van Nostrand, 1950).
- ³⁸ Note that both mechanisms, TST torque and LSI effective field, may act due to the same sd exchange interaction between mobile electron spins and bound electrons providing the lattice magnetization,²⁷ but TST and LSI are the different ways of the action. It will be treated further in more detail.
- ³⁹ We mean lattice of magnetic ions taken in the continuum media approximation.
- ⁴⁰ We consider sd interaction similar for magnetic impurities and for proper magnetic ions of the lattice. The difference might arise due to spatial distributions only: random or periodic one. But all the distributions become identical in the continuum approximation.
- ⁴¹ The term “spin injection” for a disturbance of spin equilibrium by light (see, e.g., Ref. 34) or current is a traditional one starting from the first papers^{35,36} and it corresponds closely to the famous term “charge injection” in semiconductor physics.³⁷